Infrared properties of $YBa_2Cu_3O_7$ and $Bi_2Sr_2Ca_{n-1}Cu_nO_{2n+4}$ thin films

A. El Azrak and R. Nahoum
Laboratoire d'Optique Physique, Centre National de la Recherche Scientifique, Ecole Supérieure de Physique et de Chimie Industrielles de la Ville de Paris, 10 rue Vauquelin, 75231 Paris Cedex 05, France

N. Bontemps
Laboratoire de Physique de la Matière Condensée, Centre National de la Recherche Scientifique, Ecole Normale Supérieure, 24 Rue Lhomond, 75231 Paris Cedex 05, France

M. Guilloux-Viry, C. Thivet, and A. Perrin
Laboratoire de Chimie du Solide et Inorganique Moléculaire, Université de Rennes I, 35042 Rennes Cedex, France

S. Labdi, Z. Z. Li, and H. Raffy
Laboratoire de Physique des Solides, Université Paris-Sud, 91405 Orsay Cedex, France
(Received 29 September 1992; revised manuscript received 13 December 1993)

We report room-temperature optical reflectivity and transmission measurements on a variety of $YBa_2Cu_3O_7$ and $Bi_2Sr_2Ca_{n-1}Cu_nO_{2n+4}$ thin films in the 500–25 000 cm^{-1} frequency range. Reflectivity data when not biased by the substrate are used to compute the optical conductivity. A comparison of our results with published reflectivity data on single-domain $YBa_2Cu_3O_7$ crystals suggests an overwhelming contribution of the CuO_2 planes (with respect to the chains) to the optical conductivity. The data can be analyzed in terms of a Drude low-frequency contribution and a so-called midinfrared band. However, the anomalous infrared response appears to be uniquely described by a generalized Drude response: for all the samples investigated, the relaxation rate (which increases linearly with frequency) and the effective mass are found to be the same as a function of frequency.

I. INTRODUCTION

The understanding of the infrared response of high-critical-temperature copper-oxide superconductors in their normal state is still controversial. As earlier pointed out by Timusk and Tanner,[1] the infrared (IR) response may be characterized by two contributions: a low-frequency, Drude-like behavior assigned to free carriers, and a strong midinfrared contribution (the midinfrared band or MIB).[2,3]

There is clear experimental evidence in $La_{2-x}Sr_xCuO_4$ (Refs. 4 and 5), $YBa_2Cu_3O_{6+x}$ (Refs. 3, 6, and 7), $Nd_{1+y}Ba_{2-y}Cu_3O_{6+x}$ (Ref. 7), and $Bi_2Sr_2CaCu_2O_8$ (Ref. 8) that as a whole the MIB is a spectral feature associated with the presence of free carriers within the conductive CuO_2 planes. Experimentally, a chain contribution was claimed to be found in single-domain crystals (1:2:3 compounds) lying in the midinfrared range[9,10] by separating the b conductivity (contributed by both chains and planes) from the a conductivity (contributed only by plane).[11] Indeed, the reflectivity spectra do show a definite different response when the electric field is parallel or perpendicular to the chains. Although the so-called chain conductivity appears not to be negligible at all in such single-domain crystal data, we believe that these results are not necessarily contradictory with our claim that in the thin films the MIB is solely associated with the carriers within the planes, as discussed below.

The generalized Drude conductivity where both the effective mass and the relaxation time of the normal-state carriers are frequency dependent[12] appeared first as an alternative description of the infrared response. It has been promoted later through experimental analyses[13,14] showing that the relaxation rate exhibits a linear variation with frequency in a large frequency domain, up to 2000 cm^{-1} on the single-domain $YBa_2Cu_3O_7$ crystal published data,[14] and even up to 6000 cm^{-1} on Bi-based single crystals.[15] This linear frequency dependence is the counterpart of the linear temperature decrease of the normal-state resistivity in high-T_c superconductors.

This assumption has since found both experimental and theoretical support. The experimental support arises through the close relationship that exists between the MIB and the low-frequency free carrier response.[3–7] Such a description indeed assigns the entire IR response to the carriers. The theoretical background relies on the properties of the marginal-Fermi-liquid theory where scattering occurs from a flat frequency spectrum,[16] or on the properties of nesting.[17]

Our paper concentrates on room-temperature reflectivity data on a set of $YBa_2Cu_3O_7$ and $Bi_2Sr_2Ca_{n-1}Cu_nO_{2n+4}$ thin films, some of them of very high quality, in order to discuss the most relevant description of the optical conductivity.

We observe that the reflectivities and the infrared conductivities of our identified best $YBa_2Cu_3O_7$ and $Bi_2Sr_2CaCu_2O_{8+\delta}$ samples exhibit quantitatively the same frequency dependence and are very high compared to the reflectivity and optical conductivity associated to the a axis in the case of untwinned $YBa_2Cu_3O_7$ crystal.

We find that although a "two-component" picture may be used successfully in order to parametrize the optical conductivities, leading to reasonable parameters, the generalized Drude model yields a variation versus frequency of the relaxation rate and of the effective mass which shows in a broad energy range (500–6000 cm^{-1}) a *strikingly similar behavior for all the compounds studied.*

II. THIN-FILM CHARACTERISTICS

The thin films that we have studied are labeled from *A* to *F*, as follows. *A*1, *A*2: $YBa_2Cu_3O_7/MgO$, thickness 3000 Å and 2500 Å, *B*: $YBa_2Cu_3O_7/SrTiO_3$ thickness 1000 Å, *C*: $YBa_2Cu_3O_7/MgO$ thickness 500 Å, *D*: $GdBa_2Cu_3O_7/MgO$ thickness 2000 Å, *E*: $Bi_2Sr_2Ca_2Cu_3O_{10}/MgO$ thickness 3000 Å, *F*: $Bi_2Sr_2Ca_1Cu_2O_8/MgO$ thickness 3500 Å.

The details of the deposition procedure of the "1:2:3" thin films have been reported elsewhere.[18,19] Briefly, *A*, *B*, and *C* samples have been deposited *in situ* by laser ablation, using a XeCl excimer laser, at a temperature in the range 720–750 °C, under an oxygen pressure of ~0.3 mbar. The $GdBa_2Cu_3O_7$ thin film (sample *D*) has been deposited *in situ* by dc sputtering at ~700 °C, under a mixture of argon (90%) and oxygen (10%) in a high total pressure close to 1.2 mbar.

All these films have been structurally characterized by θ–2θ x-ray diffraction, which has clearly shown their *c*-axis orientation. The rocking curves (*q* scans) are narrow, typically the full width at half maximum is close to 0.5°, characteristic of the good crystallinity of the samples. The laser ablated films have been in-plane characterized by reflection high-energy electron diffraction, which gave evidence of the epitaxial growth, i.e., the axes of the films are aligned with those of the substrate.[18]

The superconducting properties of the "1:2:3" laser-ablated films have been determined by resistive or inductive measurements. Typical $YBa_2Cu_3O_7$ thin films with narrow transitions ($\Delta T < 0.5$ K) with $T_{c0}(R=0)$ up to 90 K are obtained, but for films deposited on MgO, T_{c0} lies routinely in the range 85–88 K (measured during rapid cooling). For this work, samples with various thicknesses and T_{c0} as close as possible one to the other (85.2–86.5 K) have been selected. A typical resistive transition (sample *A*) is shown in Fig. 1. Precise knowledge of the resistivity would require patterning of the films, which then precludes the optical studies. Samples prepared in similar conditions have been measured and exhibit typical resistivities of 300–400 $\mu\Omega$ cm at room temperature.

The $GdBa_2Cu_3O_7$ dc sputtered film has a narrow ($\Delta T < 0.5$ K) albeit lower transition ($T_{c0}=79.5$ K) in spite of a high quality of crystallization. This lower T_{c0} is due to the presence of a few percents of strontium impurities coming from the baryium carbonate (analytical reagent grade) precursor which has been used for the target fabrication, whereas the $YBa_2Cu_3O_7$ targets have been made from a highly purified $BaCO_3$.

The $Bi_2Sr_2Ca_{n-1}Cu_nO_{2n+4}$ thin films were deposited on single-crystal MgO (100) substrates by a sputtering technique.

The *E* sample, mainly composed of 2:2:2:3 ($n=3$) phase, was obtained in a two-step process:[20] (i) deposition on a substrate at room temperature by dc triode sputtering in pure Ar atmosphere, from a single, lead-doped target; (ii) post deposition annealing for 16 h at 857 °C in a lead-enriched atmosphere. X-ray studies of samples prepared in this way with thickness larger than 2000 Å showed that they are composed of 75–80 % of the 2:2:2:3 phase and 20–25 % of the 2:2:1:2 phase. The *E* sample is highly *c*-axis oriented. Its cationic composition determined by energy dispersion x-ray (EDX) analysis, is close to 2:2:2:3 with a partial substitution (~20%) of Pb for Bi. Its critical temperature $T_c(R=0)$ is 106 K and the resistivity at 300 K is (500±100) $\mu\Omega$ cm.

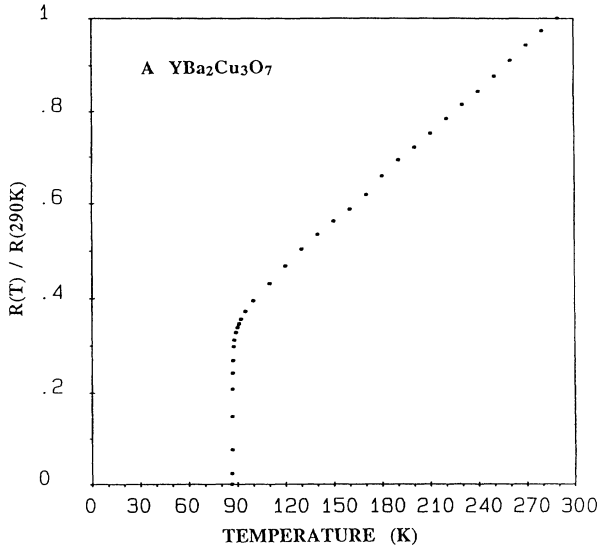

FIG. 1. Resistive transition of the $YBa_2Cu_3O_7$ *A* thin film.

The *F* sample ($n=2$) was prepared in a one-step process:[21,22] It was epitaxially grown *in situ* by rf magnetron-single target sputtering on a substrate kept at high temperature (~735 °C). The ratio Ar/O_2 of the process gas was close to 1 and the total gas pressure was 300 mTorr. The critical temperature $T_c(R=0)$ is 80 K. X-ray studies of such films showed that they are highly *c*-axis oriented and epitaxially grown.[21] The resistivity at 300 K was found to be (300±50) $\mu\Omega$ cm.

The 2:2:1:2 *F* sample has a somewhat large transition ($\Delta T \sim 10$ K). The 2:2:2:3 *E* sample has a narrower transition ($\Delta T \sim 4$ K).

III. EXPERIMENT

Reflectivity near normal incidence and transmission spectra have been recorded in the 500–7000 cm^{-1} spectral range (actually, transmission data only start at 1000 cm^{-1} due to the MgO absorption, or "reststrahlen" band, below this range) with an IFS66 Bruker Fourier-transform spectrometer and in the 5000–25 000 cm^{-1} range with a Cary 17 spectrophotometer.

All films have been studied in reflectivity, whereas only *A*, *C*, and *E* have been studied by transmission, the others exhibiting nonpolished rear face. The reflectivity spectra are displayed in Fig. 2. The *A*1 and *A*2 spectra

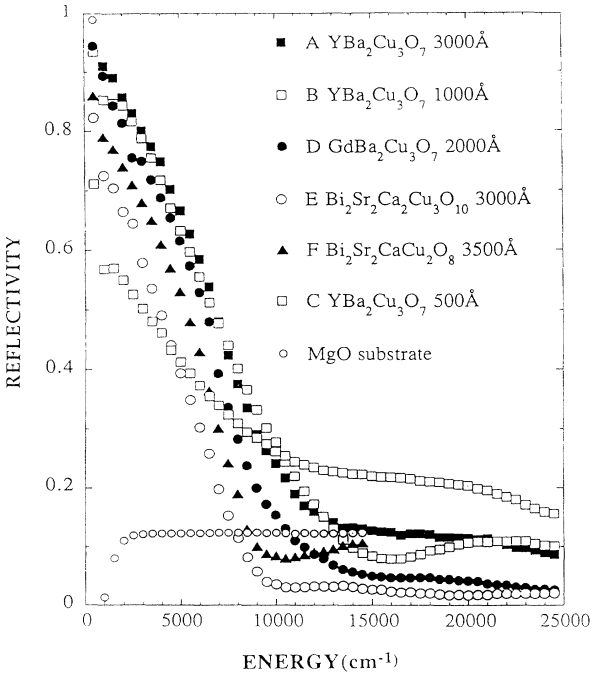

FIG. 2. Room-temperature reflectivity spectra for the set of thin films and for the MgO substrate of the *C* sample.

cannot be distinguished and therefore only the *A*1 is shown (henceforward *A*).

Transmission spectra of the *A*, *E*, and *C* films are shown on Fig. 3. The 2:2:2:3 (*E*) transmission is higher (for the same thickness) than the 1:2:3 (*A*) transmission. It is comparable to the 2:2:1:2 transmission which was measured earlier.[23] An interesting remark then arises when looking at the sample 1:2:3 (*C*) transmission, namely that decreasing the thickness by a factor of ~6 increases the transmission by a factor of ~20. This yields a valuable increase in sensitivity when looking at the temperature variation of the infrared response[24] with respect to the most appropriate free standing single crystals, namely the Bi-related family[25,26] where transmission does not exceed a few percent.

Kramers-Krönig (KK) analysis from reflectivity data (which extends towards the lowest frequency) has been used in order to establish the dielectric functions and the real part of the conductivity for a number of these samples. In order for this analysis to be valid, we have to assume that there is no significant contribution from the substrate to the reflected flux. In order to check this assumption, we first observe that the 3000 and 2500 Å (*A*1 and *A*2 films) exhibit the same reflectivity, hence the substrate contribution is indeed negligible. Kramers-Krönig transform run on these films provide the real and imaginary parts of the optical index, from which one can estimate the depth over which the light is damped by a $1/e$ factor: We find approximately 1000 Å in the whole infrared range. This means that the first reflection from the rear substrate-film interface in samples thicker than 1000 Å is damped up to 90%. Therefore for samples *D*, *E*, and *F*, the contribution of the substrate through multiple reflections is expected to be small, while it may not be the case for sample *B* and is definitely not the case for sample *C*.

Indeed note that the reflectivity spectrum of pure MgO exhibits a pronounced dip at 1000 cm^{-1} and that the same dip is clearly displayed on film *C* reflectivity: The underlying MgO substrate clearly interferes with the reflectivity of the film (see Fig. 2). Note also that the *B* sample (1000 Å thick) exhibits a similar slight dip at 1000 cm^{-1}, hence at the same frequency as the one observed on the *C* sample (500 Å thick) which may be due to the substrate. The *E* sample (3000 Å) also exhibits a very small structure: This observation is consistent with the fact that the transmission for the Bi-based materials is higher than for $YBa_2Cu_3O_7$. For the latter two films, the dip is small compared to the overall reflectivity and appears to distort only slightly the reflectivity, e.g., of sample *B* with respect to sample *A*.

We have therefore decided to run the Kramers-Krönig analysis from reflectivity spectra for samples *A*, *B*, *D*, *E*, and *F*. We shall come back to this point later and show that the assumption that the dip may be neglected for *B* and *E* is quantitatively justified.

We have chosen the Hagen-Rubens relation to extrapolate the low-frequency data, as commonly done.[3,13] The high-energy termination is more delicate. Although appending the current spectrum with high-frequency data[13]

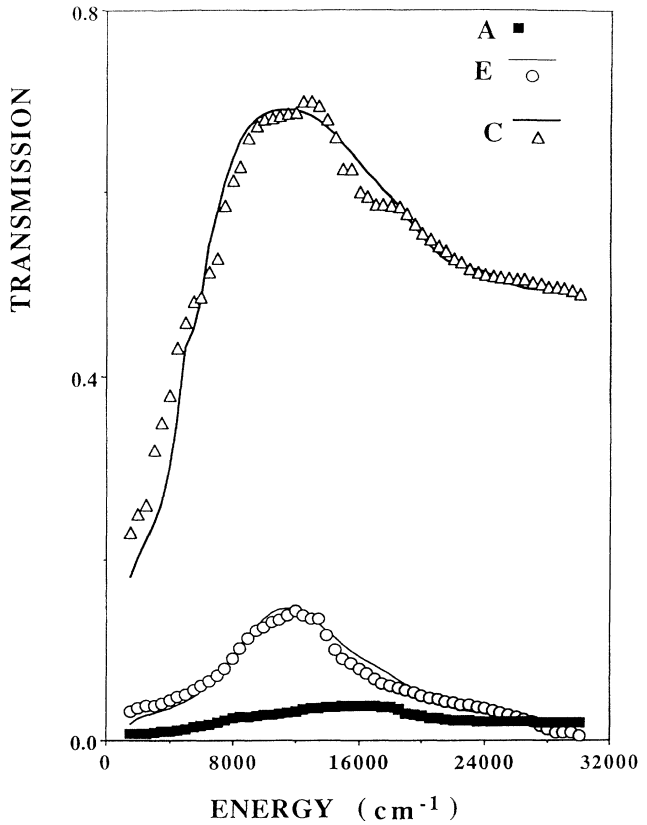

FIG. 3. Transmission spectra for the *A*, *E*, and *C* films. The solid lines are the computed spectra with the parameters shown in Table I.

may appear safer than an analytic termination, a comparison of the computed conductivities on similar twinned $YBa_2Cu_3O_7$ single crystals[3,13] with completely differing high-frequency terminations do not exhibit noticeable differences. It is easy to show that the contribution to the phase $\theta(\omega_i)$ arising from the $\omega \gg \omega_i$ frequencies involves a term of the order of ω_i/ω and therefore decreases strongly any weight due to the actual high-frequency reflectivity. Finally, combining ellipsometric and reflectance data in order to reduce the uncertainties due to the terminations[27] is certainly desirable but not always available.

We have then assumed for the high-frequency termination $\omega > \omega_{max}$

$$R(\omega)=R(\omega_{max})(\omega/\omega_{max})^p , \quad (1)$$

and we have adjusted the p exponent in order to fit smoothly the reflectivity spectrum.

Figure 4 displays the real and imaginary parts of the dielectric function for the A, B, D, E, and F samples:

$$\varepsilon(\omega)=\varepsilon_1(\omega)+i\varepsilon_2(\omega) . \quad (2)$$

Figure 5 shows the real part $\sigma_1(\omega)$ of the optical conductivity for the same samples. We show in Fig. 6 the conductivity for the A sample in a restricted frequency range 500–8000 cm^{-1} in order to compare to single-domain crystal data.[14]

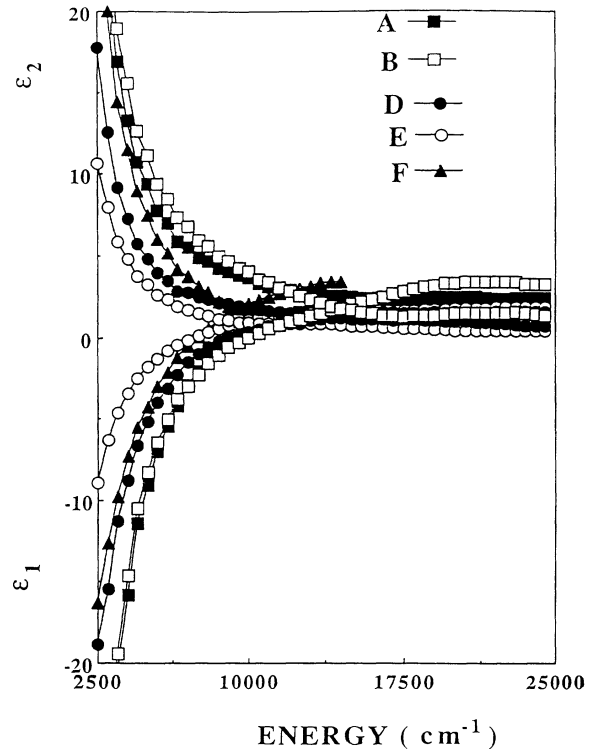

FIG. 4. Real and imaginary parts of the dielectric function versus frequency obtained by Kramers-Krönig transform of the data of Fig. 2. The lines are the best fits to Eq. (4), using the parameters from Table I.

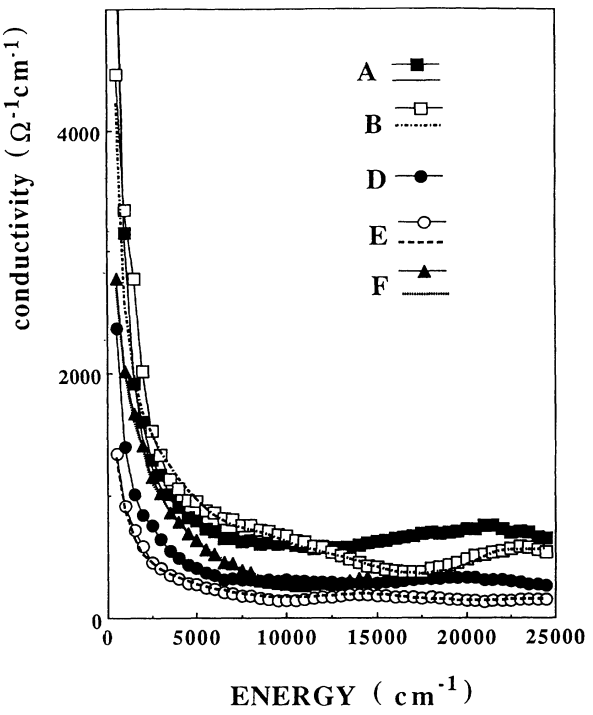

FIG. 5. Real part of the conductivity for the same set of samples as in Fig. 3. The lines are the best fits to Eq. (4), using the parameters from Table I.

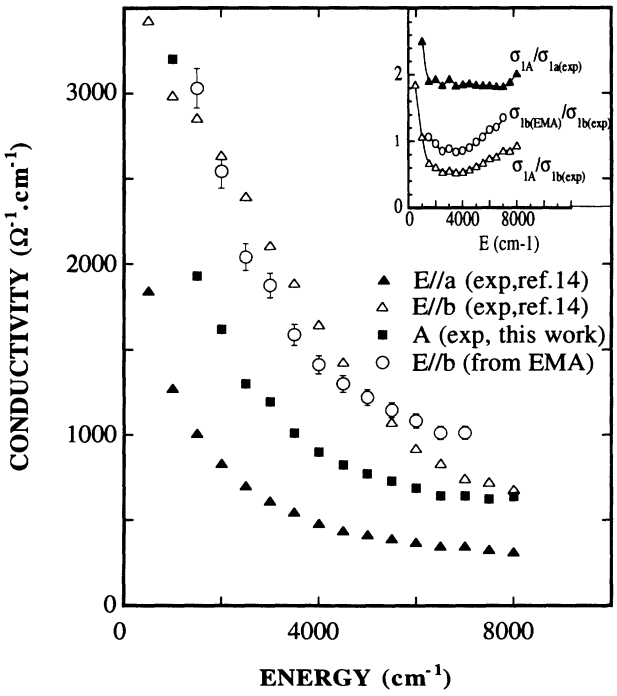

FIG. 6. A comparison between the real part of the conductivity along the a and b directions in an untwinned crystal (Ref. 14), the A conductivity and the EMA computed conductivity along b which would yield the experimentally measured A conductivity (see text). Inset: ratios σ_{1A}/σ_{1a} (full triangles), σ_{1A}/σ_{1b} (open triangles), $\sigma_{1b(cal)}/\sigma_{1b(exp)}$ (open circles)

A. Raw spectra

The comparison with earlier twinned single crystals shows that our data (for the A and B films, despite the dip at 1000 cm^{-1} for the latter) lie above those for twinned single crystals. Indeed, the data of Ref. 3 [recorded at 100 K, which increases the reflectivity by $\sim 4\%$ (Ref. 13)] are comparable to B, and the data of Ref. 13 (250 K) are comparable to D. From this point of view, this shows that our films are of better quality than those single crystals.

A comparison of the reflectivity of sample A and B to the published reflectivity of an untwinned $YBa_2Cu_3O_7$ crystal for the electric field polarized either parallel to the a axis ($E \| a$, likely probing the CuO_2 planes) or parallel to the b axis ($E \| b$, likely probing both planes and chains)[14] shows that the reflectivity of the A and B films lies in between the $R \| a$ (R_a) and $R \| b$ (R_b) spectra above 3000 cm^{-1}.

According to current undergoing investigation, epitaxial films develop domains with an approximate 1000-Å size, each of those having the a or b axis parallel to one side of the substrate,[19] and could be untwinned due to their small size.[28] In order to discuss the unpolarized light reflectivity data, one can choose to analyze the unpolarized light along the perpendicular sides of the substrate. Therefore one expects the same averaging of the a and b response for each independent polarization. The proper way then to approach this problem is first to distinguish between the range where the size D of the domains $\| a$ and $\| b$ is large compared to the wavelength of the incident light, and the range where this characteristic size D is small compared to the wavelength. This defines a crossover wavelength of ~ 1000 Å, e.g., an energy of 100 000 cm^{-1}. According to this figure, the conventional optical spectral range is in the regime where the wavelength is long compared to the typical size of the domains. Note that the orthogonal twinned structure in a single crystal is different from the possibly alternating a and b orientations of the microcrystals in an epitaxial film: One gets twin boundaries at a typical $\sim 500-1000$ Å distance;[29] again this domain size is small compared to usual wavelengths.

In the opposite case, it would be natural to identify our spectrum to an averaged spectrum

$$\langle R \rangle = 1/2(R_a + R_b) . \tag{3}$$

We have done it for the matter of the comparison: $\langle R \rangle$ coincides almost perfectly with our reflectivity above 5000 cm^{-1} but clearly drops below it in the 1500–4000 cm^{-1} range, reaching $\sim 4-6\%$ difference. Note that this comparison has been done between room-temperature spectra (ours) and 100-K spectra[14] where the reflectivity is expected to be slightly enhanced,[12] therefore we may minimize the observed difference.

One could then argue from the good agreement between $\langle R \rangle$ and the films or twinned crystals reflectivity in the midinfrared that the crossover from wavelength short with respect to the size D of any domains to wavelength long with respect to D occurs around 2 μm. However, in the case of films as well as single crystals, these sizes are definitely much smaller. Moreover, the film reflectivity is systematically higher than R_a or R_b in the infrared (< 5000 cm^{-1}).

Therefore, we think that the reflectivity measured on our films cannot be the simple average of the $R \| a$ and $R \| b$ reflectivities. The search for another kind of averaging, in the alternate limit where the wavelength is large compared to the domain size, has to be performed using the conductivity. This is discussed in Sec. III C1.

The $Bi_2Sr_2Ca_2Cu_3O_{10}$ and $Bi_2Sr_2Ca_1Cu_2O_8$ thin films do not exhibit a reflectivity as high as $YBa_2Cu_3O_7$ compounds. To our knowledge, there are less published data in a wide spectral range on these systems than on $YBa_2Cu_3O_7$. Below 4000 cm^{-1}, the single crystals exhibit a slightly higher reflectivity.[8,30] Late work reports the transmission spectra of single crystals.[25,31] Therefore we shall only be able to compare below the optical conductivities. The 2:2:2:3 spectrum is similar to the 2:2:1:2 one but the low reflectivity in the visible range is a clear indication of surface degradation. It got slightly deteriorated with time, which tended to decrease the reflectivity by $\sim 10\%$.

B. Dielectric function

1. The MIB model

In order to interpret quantitatively the spectra, we have first fitted the real and imaginary part of the dielectric function (computed through KK transform) for samples A, B, D, E, and F, to a phenomenological model, writing the dielectric function as follows:

$$\varepsilon(\omega) = \varepsilon_\infty - \frac{\omega_p^2}{\omega(\omega + i\gamma)} + \sum_i \frac{\omega_{fi}^2}{\omega_i^2 - \omega^2 - i\omega\gamma_i} , \tag{4}$$

where ε_∞ is the dielectric constant comprising the high-frequency electronic contributions, ω_p is the plasma frequency, γ is the relaxation rate, ω_{fi} the oscillator strength of the ith Lorentz oscillator, ω_i its central frequency, and γ_i its damping factor. The parameters that we find are gathered in Table I. The computed dielectric functions are the lines shown in Fig. 4.

One single value for the plasma frequency (12 000 cm^{-1} or 1.5 eV) for the A and B $YBa_2Cu_3O_7$ compound has been used to fit all the $\varepsilon_1(\omega)$ and $\varepsilon_2(\omega)$ curves; however, sample D requires a somewhat smaller value (11 000 cm^{-1}): As mentioned in the second paragraph, this sample contains strontium impurities and exhibits a lower T_c.

We find also a lower value for the Bi compounds (8000 cm^{-1}). These values are in reasonable agreement with what is now commonly found when such an analysis is performed.[3,23,25] We find as usual a very large Lorentz oscillator in the midinfrared range (the midinfrared band or MIB). A number of oscillators in the visible range are identified but their weight cannot be precisely determined and may be accounted for by ε_∞.

We have also reported in Table I the dc resistivity ρ_{opt} that can be inferred from this fitting procedure, which is computed in cgs units from

$$\rho_{opt} = 62\frac{\gamma}{\omega_p^2} , \tag{5}$$

TABLE I. Best values for the most relevant parameters of the two-component model according to Eq. (4). e_s and e_f are the substrate and film thicknesses.

	ε_∞	γ (cm^{-1})	ω_p (cm^{-1})	ω_{MIB} (cm^{-1})	ω_f (cm^{-1})	γ_{MIB} (cm^{-1})	e_s (μm)	e_f (Å)	ρ_{opt} $\mu\Omega$ cm
A	4	450±50	12 000 ±500	1000	20 000	8000	500	3000±200	195±25
B	4.3	700±100	12 000 ±500	1000	23 000	6000	500	1000	300±50
C	4	450±50	12 000 ±500	1300	20 000	3000	500	500±50	195±25
D	3	500±100	11 000 ±500	1000	15 000	7000	500	2000	250±50
E	3	900±100	8250±250	1000	12 000	7000	600	3000	900±100
F	4.5	450±100	8000±500	1000	18 500	5000	600	3500	450±150

where ω_p and γ are in cm^{-1}. The actual dc resistivities of the various samples have been indicated in the paragraph dealing with the sample characteristics

Because of the uncertainties on the determination of ω_p and γ through our fitting procedure, it is clear that one can only find approximate values for ρ_{opt}. They range between 200 and 300 $\mu\Omega$ cm for the $YBa_2Cu_3O_7$ films, which compare satisfactorily with the dc typical values. The agreement is not so good for the Bi compounds. Concerning the raw data, the optical conductivity at the lowest frequencies for sample *B* reaches twice the dc value; for the other samples (*A*,*D*,*E*,*F*), the figures that we find for the experimental optical conductivities are compatible with dc conductivities (Fig. 5).

A consistent and independent check of the procedure is to compute the transmission of the film on its substrate with the parameters that we have obtained using only the reflectivity data and their KK transform. We recall that in order to do so, we have for each film measured the transmission and reflection spectrum of the MgO substrate from the same origin; we then determine the optical constants of this particular substrate in order to compute the full transmission, by modeling multiple reflections *within the film and the substrate.*[24,32]

The results of the calculation are shown in Fig. 3 by the solid lines. The experimental spectra for the *A* and *E* samples agree with the computed ones using the parameters defined by the best fit to the dielectric constant.

In the case of the $YBa_2Cu_3O_7$ *C* (500 Å) sample, the procedure was different because the role of the substrate is definitely extremely important. We have adjusted the parameters in order to fit simultaneously the reflectivity and transmission, including for both multiple reflections in the film and the substrate. Fitted spectra are shown in Fig. 3. It turns out that it is not possible to fit simultaneously the reflectivity and transmission spectra of this thinner film with the parameters used for the other thicker films. In particular, the width of the MIB is 3000 cm^{-1} instead of 8000 cm^{-1} (Table I) and there is the need for an extra band at 7500 cm^{-1} to fit the near infrared spectrum. Technically, this change in parameters is required in order to account for the "dip," due to the substrate, that now affects strongly the reflectivity and which is not properly taken into account even when modeling the substrate effect. This may be related to the fact that the substrate undergoes a rapid change of its optical constants due to the reststrahlen band (Fig. 2).

The above comparison of the phenomenological parameters which account for the reflectivity and transmission spectra of films of various thicknesses can be taken as an indication of the effect of the substrate as a function of thickness. Up to 1000 Å, for $YBa_2Cu_3O_7$ films, the role of the substrate cannot be neglected. At 1000 Å (*B*), it does distort (through a slight dip) the spectrum: This bears some consequences for the conductivity (which is indeed for instance too high at low frequency, as mentioned) and the relaxation rate, as will be shown further. However, if one simply neglects this dip, the parameters that fit the spectra are the same as for thick samples. This suggests that indeed the effect is almost negligible. The 2500- and 3000-Å spectra are identical and are smooth at 1000 cm^{-1}. The *A* spectrum is from this respect the most reliable.

We are going to analyze the *A*, *B*, and *D* conductivities, bearing in mind that the *B* and *D* ones may be slightly distorted around 1000 cm^{-1} but not otherwise. We shall apply the same conclusions to the *E* and *F* films, relying on the fact that the dip when present is comparable to the one observed on the *B* and *D* samples.

2. The layered electron gas

It has been argued, relying essentially on the experimental observation that the frequency dependence of $\mathrm{Im}(-1/\varepsilon)$ is quadratic, that the non-Drude behavior may be characteristic of a layered electron gas and that the relevant variable is the density of carriers per "slab," one slab being a set of CuO_2 monolayers.[27,33,34]

We have reported $\mathrm{Im}(-1/\varepsilon)$ versus frequency in a ln-ln plot (Fig. 7). We get reasonable straight lines up to 3800 cm^{-1}, defining an exponent 1.8±0.2, consistent with a quadratic behavior:

$$\mathrm{Im}(-1/\varepsilon)=\beta\omega^2 . \quad (6)$$

The value of β changes by ~ 2 from one sample to the other, as already noticed.[34] We do not observe any linear dependence of the critical temperature T_c versus the slab carrier density d/β as found previously.[34] Therefore we

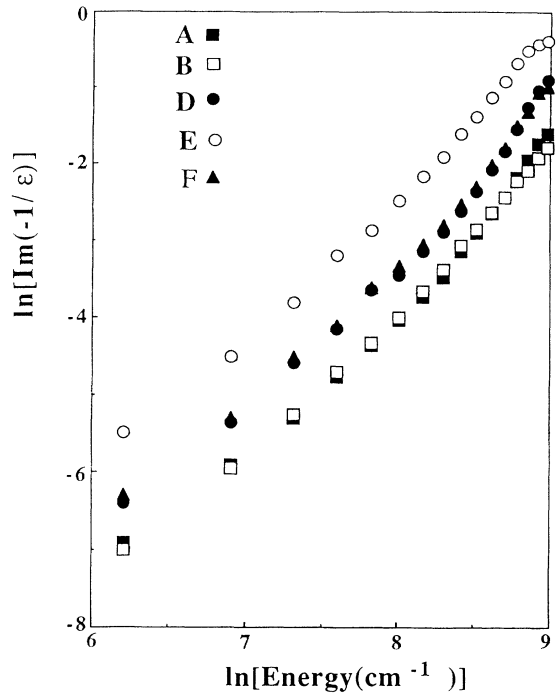

FIG. 7. Ln-Ln plot of $\mathrm{Im}(-1/\varepsilon)$ versus frequency for the various samples.

do not believe that this description provides a unified picture for the cuprate superconductors.

C. Real part of the conductivity

The real part of the conductivity will be henceforward identified as σ_1 and the imaginary part by σ_2.

1. Comparisons with single crystals

For the $Bi_2Sr_2CaCu_2O_{8+\delta}$ films, the conductivity is different and larger than the single crystals' conductivities available at room temperature although the reflectivity is either lower (below 4000 cm^{-1}) or the same.[30,31]

For $YBa_2Cu_3O_7$ films, we have compared the real part of the conductivities represented on Fig. 5 to a few published conductivity data on $YBa_2Cu_3O_7$ single crystals.[3,13,14] We perform our comparison between 1000 and 8000 cm^{-1}, because this part of the spectrum does not depend very much on temperature and that all the published data are not available at room temperature.

The *A* and *B* films and the twinned crystals[3,13] exhibit a quite similar *ab* plane conductivity. In particular the 1000 cm^{-1} points all lie between 2500 and 3200 $\Omega^{-1}cm^{-1}$ and the overall conductivities never depart from each other by more than 200 $\Omega^{-1}cm^{-1}$. On the contrary, as could be expected from the above discussion on the reflectivity spectra themselves, there is a clearcut difference between our experimental conductivities and the *a* and *b* conductivities, as shown in Fig. 6. As could be expected, the film (and twinned crystal) conductivity lies in between σ_{1a} and σ_{1b} except for the far infrared (<1000 cm^{-1}), suggesting that the effective conductivity is some average of σ_a and σ_b. The point is to know what kind of an average yields our measured conductivity σ. (This problem is also pendent for the twinned crystals.)

An appealing solution would be to call for an effective-medium approximation (EMA) in order to compute the effective conductivity σ_m in the case where the wavelength is large compared to the characteristic size of the domains. As a model calculation, we choose here the approach of Landauer in a binary metallic mixture,[35] which is, however, meant for dc conductivities. As already stated, the unpolarized light data can be represented by summing over two contributions of the electric field, one associated with a polarization parallel to one side of the film, one parallel to the other side. Along each of these directions, we assume domains which exhibit at random σ_a and σ_b conductivities.

We follow the same line of calculation as Landauer, but consider an arbitrary shape associated with a N depolarizing factor ($N=\frac{1}{3}$ for a sphere). Indeed, each domain is approximately $1000\times1000\times d$ Å^3, where d is the thickness of the film. The effective conductivity is then defined by the equation:

$$\frac{\sigma_a-\sigma_m}{N\sigma_a+(1-N)\sigma_m}+\frac{\sigma_b-\sigma_m}{N\sigma_b+(1-N)\sigma_m}=0\ . \tag{7}$$

As noticed by Stroud,[36] these calculations apply to the complex conductivity. Therefore if we wish to compute the real and imaginary part of σ_m, we must use both the real and imaginary parts of σ_a and σ_b (σ_{1a} and σ_{2a}, σ_{1b} and σ_{2b}) possibly extracted from single-domain crystal data: only their real parts have been published.[14] In order to overcome this difficulty, we have taken advantage of our experimental observation that in the 1000–7000 cm^{-1} frequency range:

$$\sigma_{1A}=(1.8\pm0.01)\sigma_{1a}\ . \tag{8}$$

We show the ratio σ_{1A}/σ_{1a} in the inset of Fig. 6, together with the ratio σ_{1A}/σ_{1b}. Because σ_{1a} and σ_{1b} are linearly related through the Kramers-Krönig relation, we infer from Eq. (8) that

$$\sigma_{2A}=(1.8\pm0.01)\sigma_{2a}\ . \tag{9}$$

If the EMA description holds for the thin film, e.g., *A*, then we should have

$$\sigma_m=\sigma_{1m}+i\sigma_{2m}\equiv\sigma_{1A}+i\sigma_{2A}\ . \tag{10}$$

Using then $\sigma_{1A}+i\sigma_{2A}$ for $\sigma_{1m}+i\sigma_{2m}$, and $\sigma_{1a}+i\sigma_{2a}$ derived from Eqs. (8) and (9), one can compute $\sigma_{1b}+i\sigma_{2b}$ from Eq. (7). We have done so, taking $N\sim\frac{1}{3}$ (the penetration depth of the light is ~1000 Å in the infrared hence the domains are roughly cubic). We then compare the computed conductivity $\sigma_{1b(\mathrm{EMA})}$ to the experimental conductivity $\sigma_{1b(\mathrm{exp})}$.[14] The results are shown in Fig. 6, for the range where Eq. (8) is experimentally valid (1000–7000 cm^{-1}). The calculated and experimental values of σ_{1b} do not agree very well. In the inset, we show the ratio $\sigma_{1b(\mathrm{exp})}/\sigma_{1b(\mathrm{EMA})}$. This ratio should be equal to 1 if the EMA holds, and it changes its value be-

tween 0.86 and 1.35, which seems to be beyond the experimental error. Therefore we find that this EMA average of the conductivities does not work satisfactorily. This, however, only implies that this tentative EMA approach is not really adequate. The search for a more appropriate description is beyond the scope of this paper.

2. *Frequency dependence of the conductivity*

We have analyzed the frequency dependence of the conductivity of the various films as a function of frequency in the 500–8000 cm^{-1} range. We have looked for the best fit to a $\omega^{-\alpha}$ decay (Fig. 8). The exponent α is given for the various samples in Table II, together with those which we have derived for the untwinned single crystal. Satisfactory agreement with a power-law decay is obtained with all film conductivities as shown in Fig. 8. On the contrary, no satisfactory adjustment with an $\omega^{-\alpha}$ power law can be obtained with the conductivity σ_b parallel to the b axis, showing a different behavior of the conductivity along the b axis, likely due to the chains.

The striking result is that the exponent is ~0.77 for all the films, except B, for which the exponent value is lowered due to the dip. This exponent is fairly close to the one obtained for σ_{1a} from Ref. 14 ($\alpha=0.67$, Table II). For the matter of the comparison, Fig. 8 shows that σ_{1A} and $1.8\sigma_{1a}$ are indeed very close. Of course, one would find the same similarity between σ_{1a} and the conductivity for an another film, by changing the multiplying factor, since all conductivities display the same frequency variation. This observation, added to the similarity of the behavior of the $YBa_2Cu_3O_7$ and the Bi-based compounds seem to indicate that the measurements on $YBa_2Cu_3O_7$ thin films (and presumably on twinned single crystals) are insensitive to the chains contribution and arise predominantly from the CuO_2 planes. We shall bring further evidence of this point later when dealing with the relaxation rate.

3. *Relaxation rate*

The non-Drude behavior can be described, as mentioned in the Introduction, in terms of a frequency dependent relaxation rate and effective mass.[12–14] This does not call immediately for a theoretical model.

According to this generalized Drude model, we have extracted the relaxation rate for the A, B, D, E, and F samples and we show its frequency dependence in Fig. 9: *All the relaxation rates* (except the E sample which is shifted with respect to the others, most likely because the response is not the actual one) *exhibit the same linear dependence, up to very high frequencies* (*6000 cm^{-1}*), whatever the compound. The discrepancy for the B sample at 1000 and 2000 cm^{-1} corresponds to the "MgO dip." Above 6000 cm^{-1}, as can be seen in Fig. 9, the points start to depart from the straight line.

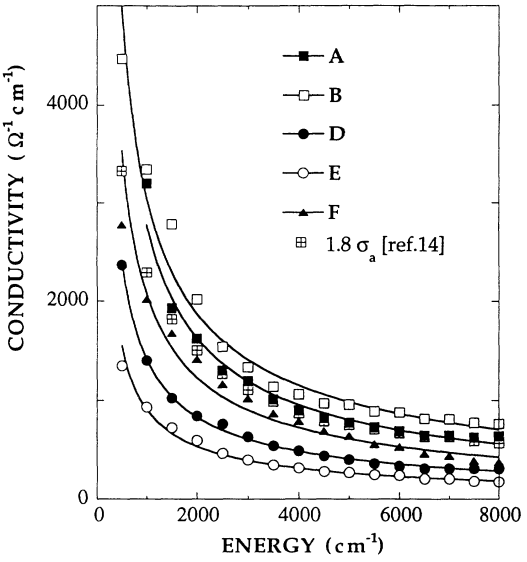

FIG. 8. Frequency dependence of the real part of the conductivity for the A, B, D, E, and F films. The solid lines show the best fit to a power-law decay $\omega^{-\alpha}$. The exponent α is given in Table II. For the sake of the comparison, we show the conductivity σ_a [conductivity measured along the a direction in an untwinned single crystal (Ref. 14)] multiplied by 1.8.

This linear dependence can be written as

$$1/\tau=(0.67\pm0.07)\omega \ . \tag{11}$$

We have also reported in Fig. 9 the points extracted under similar assumptions for the σ_a conductivity of the untwinned crystal:[14] These points fall right on top of ours. This *confirms that the chain contribution is not seen in the films.*

Finally, we show in Fig. 10 the corresponding dependence of the effective masses as a function of frequency. Again, all effective masses exhibit a similar frequency variation, confirming some kind of unique behavior for all these compounds.

An interesting question is immediately raised: Is this behavior characteristic of the cuprates or not? The

TABLE II. Values of the exponent α describing the best fit $\sigma\sim\omega^{-\alpha}$ for the various films labeled A, B, D, E, and F films. σ_a and σ_b stand for the conductivities measured along the a and b directions in an untwinned single crystal (Ref. 14). σ_{MFL} stands for the computed conductivity at 100 and 300 K for the marginal-Fermi-liquid model (MFL) (Ref. 16). The exponent is given within ±0.05.

σ_A (300 K)	σ_B (300 K)	σ_D (300 K)	σ_E (300 K)	σ_F (300 K)	σ_a (100 K)	σ_b (100 K)	σ_{MFL} (300 K)	σ_{MFL} (100 K)
0.77	0.70	0.77	0.76	0.76	0.67	none	0.74	0.68

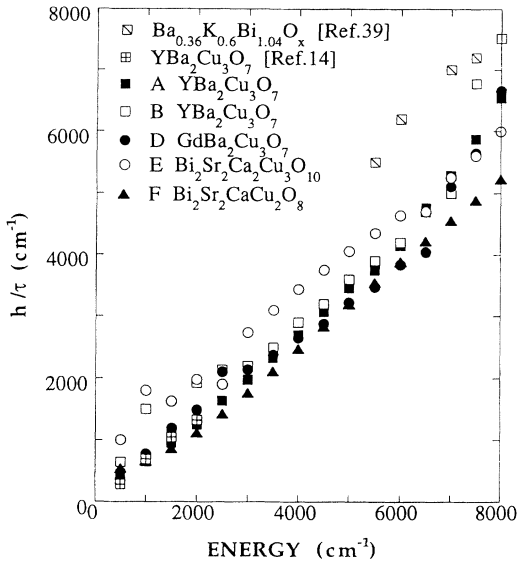

FIG. 9. Relaxation rate $1/\tau$ (or inverse lifetime) of the *A*, *B*, *D*, *E*, and *F* films computed from the dielectric functions shown in Fig. 4. The data referring to the *a* axis in an untwinned single crystal (Ref. 14) and to a $Ba_{1-x}K_xBiO_3$ film (Ref. 34) are shown for comparison.

answer to this question requires similar analysis in metallic oxides which are neither cuprates not superconductors, but do exhibit a qualitatively similar infrared behavior.[30,37,38] Unfortunately, most of the published data do not allow a quantitative comparison. We were restricted to a comparison to the $Ba_{1-x}K_xBiO_3$ case

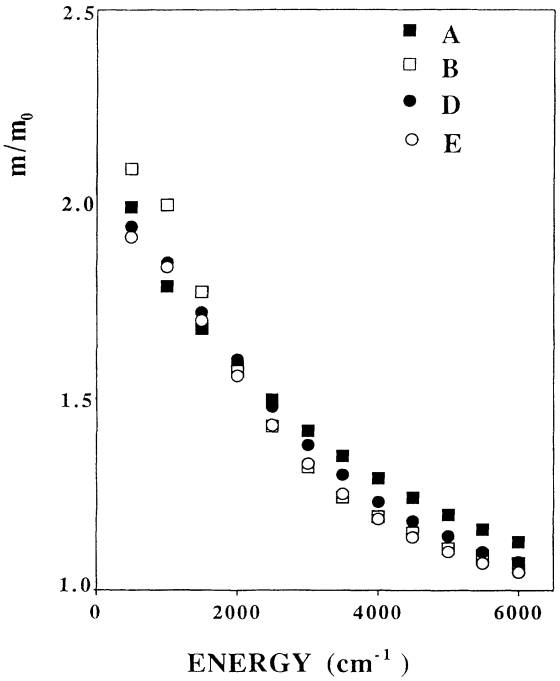

FIG. 10. Ratio of the effective mass to the bare electron mass as a function of frequency for the *A*, *B*, *D*, and *E* films.

where the dielectric functions $\varepsilon_1(\omega)$ and $\varepsilon_2(\omega)$ have been derived from reflectivity and ellipsometric data.[39] $\mathrm{Im}(-1/\varepsilon)$ is also nearly quadratic as compared with superconducting cuprates, but the relaxation rate that can be extracted using the dielectric function data appears to be much faster (the points fall more than 1000 cm^{-1} above our points). Unfortunately there are only few points available on the high-frequency side (5000–6000 cm^{-1}) and therefore such data are not accurate enough to yield a definite conclusion. These results clearly demonstrate the relevance of this analysis in order to confirm or rule out the specificity of the infrared response of the cuprate superconductors.

IV. BRIEF COMPARISON WITH THEORETICAL MODELS

There are presently several theories for cuprate superconductors which concentrate on the optical conductivity and predict an anomalous frequency dependence of the optical conductivity or a relaxation rate which varies linearly in frequency (or both).

One is the marginal-Fermi liquid (MFL), where one expects[16]

$$\hbar/\tau_{\mathrm{MFL}}=2\pi\lambda(\hbar\omega+\pi k_B T)\ , \tag{12}$$

where λ is a coupling constant. This linear dependence is expected to hold up to a cutoff frequency ω_c related to the energy spectrum of the bosonic spectrum which is flat up to this frequency. According to this prescription, the linearity domain, which we find to extend up to 6000 cm^{-1}, appears unusually large if referring to a characteristic energy scale. If we compare Eq. (12) to our data, this yields $\lambda_{\mathrm{opt}}=0.11\pm0.01$. Turning to the dc resistance measurements, and relying on the estimate of a typical dc conductivity, we derive a similar value for $\lambda_{\mathrm{tr}}=0.10-0.15$. This agreement confirms that the relaxation time measured by optical means in the midinfrared is indeed connected with the time involved in dc transport.

Concerning the conductivity, it is expected to vary as ω^{-1} in the high-frequency regime. Because our frequency range crosses the assumed cutoff frequency of Ref. 16, we directly identified the effective exponent for the computer conductivity of Ref. 16 in the 500–2000 cm^{-1} range (Table II). We note the surprisingly good agreement of this exponent and the one that we find on our films (see Table II).

The nested-Fermi-liquid model[17] or NFL yields very similar predictions. The frequency dependence of the conductivity is ω^{-1} and the relaxation rate writes:

$$1/\tau_{\mathrm{NFL}}=\alpha\max(\omega,\beta' T)\ . \tag{13}$$

β' is of the order of unity. According to Ref. 17, the cutoff frequency $\omega_c=W/(1+\alpha)$ may be very high since W is a bandwidth (of the order of eV) and α is a coupling coefficient (≤ 1). A numerical estimate of the slope of $1/\tau$ versus frequency (both calculated within the same units) is 0.79, which does compare favorably to the experimental value 0.67 ± 0.07.

Finally, gauge theories[40,41] predict that the optical con-

ductivity at high frequency should be dominated by a $T^2\omega^{-1/2}$ term.[41] Such a frequency dependence is not inconsistent with the exponent that we find, however the T^2 term looks puzzling and does not describe properly the temperature dependence.

At this point we have no real possibility to discriminate between the two models. The temperature variation of the relaxation rate in the whole frequency range would be of interest. Transmission measurements have been performed which confirm quantitatively Eq. (12) in the 500–6000 cm^{-1} range.[24]

V. CONCLUSION

We have shown that reflectivity and transmission data may now be obtained on high-quality epitaxial thin films. We have shown that these data can be used when thin films are thick enough in order to obtain the conductivity and the results can be cross checked using their transmission. Our conductivity data compare favorably with the best single-crystal data.

The fact that the optical conductivity exhibits the same frequency variation for all the compounds, and that the relaxation rate is quantitatively the same for all compounds, strongly suggests that the CuO_2 plane contribution is predominant on thin films. How this relates with the microstructure remains to be clarified. However, from a qualitative point of view, one may argue that the chains cannot be connected with one another between two domains rotated by 90°, hence cannot contribute to the conductivity for wavelengths significantly larger than the size of the domains, whereas the planes in each domain can connect one to the other. This is an important result because it validates all the data on films (and on twinned single crystals as well) as characterizing the CuO_2 plane response.

Our samples yield the same frequency dependence of the optical conductivity, well described by a power-law decay with a single exponent (-0.77). Our most striking result is that the relaxation rate is linear in frequency up to 6000 cm^{-1}, whatever the nature of the compound, in good agreement with the marginal-fermi-liquid model.

These results raise the crucial question namely the uniqueness of this behavior for cuprate oxides. Although there is some indication from the published results that indeed noncuprate superconductors exhibit a quantitative different dependence with frequency, this question remains to be settled.

ACKNOWLEDGMENTS

We are indebted to Professor A. C. Boccara for valuable help, to Professor C. Varma and to Professor P. Richards for an illuminating discussion. We thank Professor R. Combescot, Professor M. Gabay, and Professor P. Lederer for fruitful suggestions. Laboratoire d'Optique Physique is Unité Propre de Recherche du CNRS No. 005. Laboratoire de Physique de la Matière Condensée is Unité de Recherches Associée au CNRS No. 1437. Laboratoire de Chimie du Solide et Inorganique Moléculaire is Unité de Recherche Associée au CNRS No. 1495. Laboratoire de Physique des Solides is Laboratoire Associé au CNRS No. 2.

[1]T. Timusk and D. Tanner, Physica C **169**, 425 (1990).

[2]T. Timusk and D. Tanner, in *Physical Properties of High-Temperature Superconductors I,* edited by D. M. Ginsberg (World Scientific, Singapore, 1989), p. 339.

[3]J. Orenstein, G. A. Thomas, A. J. Millis, S. L. Cooper, D. H. Rapkine, T. Timusk, L. F. Schneemeyer, and J. V. Warszczak, Phys. Rev. B **42**, 6342 (1990).

[4]S. Tajima, S. Tanaka, and S. Uchida, in *Proceedings of the 2nd International Symposium on Superconductivity (ISS'89) Tsukuba,* edited by T. Ishiguro and K. Kajimura (Springer-Verlag, Tokyo, 1990).

[5]S. Uchida, T. Ido, H. Takagi, T. Arima, Y. Tokura, and S. Tajima, Phys. Rev. B **43**, 7942 (1991), p. 569.

[6]G. A. Thomas, S. L. Cooper, J. Orenstein, D. H. Rapkine, A. J. Millis, J. V. Waszczak, and L. F. Schneemeyer, Supercond. Sci. Technol. **4**, S235 (1991).

[7]J. Bouvier, N. Bontemps, M. Gabay, M. Nanot, and F. Queyroux, Phys. Rev. B **45**, 8065 (1992).

[8]J. H. Kim, I. Bozovic, D. B. Mitzi, A. Kapitulnik, and J. S. Harris, Jr., Phys. Rev. B **41**, 7251 (1990).

[9]M. P. Petrov, A. I. Grachev, M. V. Krasin'kova, A. A. Nechitailov, V. V. Prokofiev, V. V. Poborchy, S. I. Shagin, and N. F. Kartenko, Solid State Commun. **67**, 1197 (1988).

[10]J. Tanaka, K. Kamiya, and S. Tsurumi, Physica C **153-155**, 653 (1988).

[11]B. Koch, H. P. Geserich, and T. Wolf, Solid State Commun. **71**, 495 (1989).

[12]G. A. Thomas, J. Orenstein, D. H. Rapkine, M. Capizzi, A. J. Millis, R. N. Bhatt, L. F. Schneemeyer, and J. Warszczak, Phys. Rev. Lett. **61**, 1313 (1988).

[13]Z. Schlesinger, R. T. Collins, F. Holtzberg, C. Feidl, G. Koren, and A. Gupta, Phys. Rev. B **41**, 11 237 (1990).

[14]Z. Schlesinger, R. T. Collins, F. Holtzberg, C. Feild, S. H. Blanton, U. Welp, G. W. Crabtree, Y. Fang, and J. Z. Liu, Phys. Rev. Lett. **65**, 801 (1990).

[15]I. Terasaki, S. Takebayashi, I. Tsukada, A. Maeda, and K. Uchinokura, Physica C **185-189**, 1017 (1991).

[16]C. M. Varma, P. Littlewood, S. Schmitt-Rink, E. Abrahams, and A. Ruckenstein, Phys. Rev. Lett. **63**, 1996 (1989); P. B. Littlewood and C. M. Varma, J. Appl. Phys. **69**, 4979 (1991).

[17]A. Virosztek and J. Ruvalds, Phys. Rev. B **42**, 4064 (1990); J. Ruvalds and A. Virosztek, *ibid.* **43**, 5498 (1991).

[18]M. G. Karkut, M. Guilloux-Viry, A. Perrin, J. Padiou, and M. Sergent, Physica C **179**, 262 (1991).

[19]M. Guilloux-Viry, M. G. Karkut, A. Perrin, and M. Sergent, Mater. Lett. **10**, 126 (1990).

[20]S. Labdi, H. Raffy, A. Vaures, and P. Tremblay, J. Less Common Met. **164-165**, 687 (1990); S. Labdi, S. Megtert, and H. Raffy, in *Proceedings of ICAM-91 EMRS Conference, Strasbourg 1991,* edited by L. Correra (Elsevier, New York, 1992), p. 37.

[21]Z. Z. Li, S. Labdi, A. Vaures, S. Megtert, and H. Raffy, *Proceedings of ICAM-91 EMRS, Conference, Strasbourg (1991)* (Ref. 20), p. 487.

[22]Z. Z. Li, A. Vaures, S. Megtert, and H. Raffy (unpublished).

[23]J. Bouvier, N. Bontemps, A. C. Boccara, S. Labdi, and H. Raffy, J. Less Common Met. **164-165**, 1092 (1990).

[24]A. El Azrak, R. Nahoum, A. C. Boccara, N. Bontemps, M.

Guilloux-Viry, C. Thivet, A. Perrin, Z. Z. Li, and H. Raffy, J. Alloys Compounds **195**, 663 (1993).
[25]L. Forro, G. L. Carr, G. P. Williams, D. Mandrus, and L. Mihaly, Phys. Rev. Lett. **65**, 1941 (1990).
[26]D. B. Romero. G. L. Carr, D. B. Tanner, L. Forro, D. Mandrus, L. Mihaly, and G. P. Williams, Phys. Rev. B **44**, 2818 (1991).
[27]I. Bozovic, Phys. Rev. B **42**, 1969 (1990).
[28]K. Kechouane, H. L'Haridon, M. Salvi, P. N. Favennec, M. Gauneau, M. Guilloux-Viry, M. G. Karkut, C. Thivet, and A. Perrin, J. Mater. Sci. **28**, 4934 (1993).
[29]D. Favrot, M. Déchamps, and A. Revcolevschi, Philos. Mag. Lett. **64**, 147 (1991).
[30]I. Terasaki, T. Nakahashi, S. Takebayashi, A. Maeda, and K. Uchinokura, Physica C **165**, 152 (1990).
[31]D. B. Romero, C. D. Porter, D. B. Tanner, L. Forro, D. Mandrus, L. Mihaly, G. L. Carr, and G. P. Williams, Solid State Commun. **82**, 183 (1992).
[32]M. Sato, K. Nagasaka, M. Ihara, and T. Kimura, J. Phys. Soc. Jpn. **60**, 4337 (1991).
[33]I. Bozovic, J. H. Kim, J. S. Harris, and W. Y. Lee, Phys. Rev. B **43**, 1169 (1991).
[34]I. Bozovic, J. Supercond. **4**, 193 (1991).
[35]R. Landauer, J. Appl. Phys. **23**, 779 (1952).
[36]D. Stroud, Phys. Rev. B **12**, 3368 (1975).
[37]I. Terasaki, T. Nakahashi, A. Maeda, and K. Uchinokura, Phys. Rev. B **43**, 551 (1991).
[38]Y. Watanabe, D. C. Tsui, J. T. Birmingham, N. P. Ong, and J. M. Tarascon, Phys. Rev. B **43**, 3026 (1991).
[39]I. Bozovic, J. H. Kim, J. S. Harris, E. Hellman E. H. Hartford, and P. K. Chan, Phys. Rev. B **46**, 1182 (1992).
[40]N. Nagaosa and P. Lee, Phys. Rev. Lett. **20**, 2450 (1990).
[41]L. B. Ioffe and G. Kotliar, Phys. Rev. B **42**, 10 348 (1990).